Journal of Umm Al-Qura University for Applied Sciences
https://doi.org/10.1007/s43994-024-00137-x

REVIEW

Soliton solutions to a nonlinear wave equation via modern methods

Shuvo Sarker[1] · Rezaul Karim[1] · M. Ali Akbar[2] · M. S. Osman[3,4] · Pinakee Dey[1]

Received: 14 October 2023 / Accepted: 19 February 2024

Abstract

In this pioneering study, we have systematically derived traveling wave solutions for the highly intricate Zoomeron equation, employing well-established mathematical frameworks, notably the modified (G′/G)-expansion technique. Twenty distinct mathematical solutions have been revealed, each distinguished by distinguishable characteristics in the domains of hyperbolic, trigonometric, and irrational expressions. Furthermore, we have used the formidable computational capabilities of Maple software to construct depictions of these solutions, both in two-dimensional and three-dimensional visualizations. The visual representations vividly capture the essence of our findings, showcasing a diverse spectrum of wave profiles, including the kink-type shape, soliton solutions, bell-shaped waveforms, and periodic traveling wave profiles, all of which are clarified with careful precision.

Keywords Zoomeron equation · Modified $\left(G'/G\right)$-expansion method · Mathematical solutions · Nonlinear partial differential equations · Kink wave · Bell wave

1 Introduction

Albert Einstein once said, "The most incomprehensible thing about the world is that it is at all comprehensible. But how do we fully understand incomprehensible things?" In this sense, nonlinear science offers some hints[1]. The environment we live in is intrinsically nonlinear. In several scientific disciplines, such as fluid mechanics, solid-state physics, plasma physics, plasma waves, and biology, nonlinear evolution equations (NEEs) are frequently employed as models to describe complicated physical events.

Academics are currently focusing on nonlinear wave equations for the mathematical description and examination of real-world occurrences. To have a deeper understanding of actual events, the exact solutions of the conforming mathematical models should be obtained. Many scholars have worked hard to provide a universal approach to dealing with all types of NLEEs.

In particular, a variety of techniques have been used to investigate distinct physical model solutions that are modeled by nonlinear partial differential equations (NPDEs)., notably the Exp(-Phi)-Expansion method[2, 3], Bifurcation Analysis [4], the unified technique[5], Sine–Gordon expansion method [6], Kudryashov schemes [7], Jacobi elliptic task technique [8], the Jacobi elliptic ansatz technique [9], fractional iteration algorithm [10, 11], variation of $\left(G'/G\right)$ -expansion method [12], modified decomposition schemes [13], the hyperbolic and exponential ansatz method [14], natural transformation technique [15], Hirota's simple schemes [16, 17], the modified extended tanh expansion system [18], and significantly more[19–24]. Previous papers handled the solution procedure of nonlinear Riccati equations, Jimbo–Miwa equation, the Kadomtsev–Petviashvili

✉ Pinakee Dey
pinakeedey68@gmail.com

Shuvo Sarker
sarkershuvo.mbstu@gmail.com

Rezaul Karim
rezaul.math@mbstu.ac.bd

M. Ali Akbar
ali_math74@yahoo.com

M. S. Osman
msosman@uqu.edu.sa

1 Department of Mathematics, Mawlana Bhashani Science and Technology University, Tangail 1902, Bangladesh

2 Department of Applied Mathematics, Rajshahi University, Rajshahi, Bangladesh

3 M.S. Osman, Department of Mathematics, Cairo University, Cairo, Egypt

4 Mathematics Department, Faculty of Sciences, Umm AI-Qura University, Makkah 21955, Saudi Arabia

Published online: 27 March 2024

equation [25–29], more systematically and conveniently, and these solutions are close to the aforementioned equation and helped us in this study to investigate more novel soliton solutions.

In order to convey the reasonability and simplicity of the cycle, we instrument the modified $(G\prime/G)$−-expansion schemes in the current study to produce accurate solutions to the Zoomeron equation. The key advantage of this cycle over other designs is that it contributes more innovative precise solutions, including additional independent factors, and we also produce a few novel results. The exact reactions are crucial in disclosing the key element of the real events. In addition to its considerable significance, fractional order nonlinear population's particular responses.

To the best of our knowledge, modified $(G\prime/G)$−expansion method has not been previously employed in the derivation of soliton solutions for the nonlinear Zoomeron equation. To provide a visual representation, select instances are graphically illustrated through the utilization of Maple, a widely used commercial software platform. This innovative approach serves as a potent tool for generating traveling wave solutions across a broad spectrum of nonlinear partial differential equations.

2 The modified (G'/G)-expansion method

We are considering:

$$T\left(u, u_x, u_{xx}, u_t, u_{tt}, u_{xt}, ...\right) = 0, \tag{1}$$

where T is a polynomial in u.

Family I: Implement the traveling variable:

$$u = u(x,t) = u(\xi), \xi = p_3(x - Vt), \tag{2}$$

where p_3 and V are a constant to be determined later. Implementing Eq. (2) into Eq. (1), we find:

$$S\left(u, p_3u\prime, p_3^2u\prime\prime, -p_3Vu\prime, ...\right) = 0. \tag{3}$$

Family II: Considering the ansatz form:

$$u(\xi) = \sum_{i=-N}^{N} V_i\Delta^i, \tag{4}$$

where $\Delta = \left(\frac{G\prime}{G} + \frac{\lambda}{2}\right), |A_{-N}| + |A_N| \neq 0$ and $G = G(\xi)$ satisfies the equation

$$G'' + \lambda G\prime + \mu G = 0, \tag{5}$$

where $V_i(\pm 1, \pm 2, ..., \pm N)$, λ and μ are coefficient constants later. Implementing homogeneous balance principle in Eq. (3), the positive integer N can be determined. From the Eq. (5), we find that

$$\Delta = r - \Delta^2, \tag{6}$$

where $r = \frac{\lambda^2 - 4\mu}{4}$ and r is calculated by λ and μ. So, Δ satisfies (6), which produces:

Family III: By implementing Eq. (5) and Eq. (4) and Eq. (3) and collecting all terms with the same order of Δ together, the left-hand side of Eq. (3) is converted into polynomial in Δ. Equating each coefficient of the polynomial to zero, we can get a set of algebraic equations which can be solved to find the values of the studied method.

3 Application of the modified (G'/G)-expansion method

The modified (G'/G)-expansion approach is used in this subsection to solve the Zoomeron equation in the form.

$$\left(\frac{u_{xy}}{u}\right)_{tt} - \left(\frac{u_{xy}}{u}\right)_{xx} + 2\left(u^2\right)_{xt} = 0 \tag{7}$$

where u(x,y,t) is the amplitude of the relative wave mood. This equation is one of incognito evolution equation. The equation was introduced by Calogero and Degasperis [21]. Using the wave variable

$$u(x, y, t) = U(\xi), \xi = x + sy - wt,$$

Equation (7) is carried to an ODE

$$s\left(w^2 - 1\right)U\varepsilon - 2wU^3 - RU = 0, \tag{8}$$

where the prime denotes the derivation with respect to Δ and R is the integration constant.

Balancing the highest- order derivative term U'' with the nonlinear term U^3 of Eq. (8) yields N = 1 According to modified G'/G expansion method,

Now the solution of Eq. (8) is,

$$U(\xi) = V_{-1}\Delta^{-1} + V_0 + V_1\Delta \tag{9}$$

Putting Eq. (9) in Eq. (8) with the help of the proposed methods we get,

Set of solutions:

Case-1:

$$S = \pm\sqrt{\frac{R}{W(\lambda^2 - 4\mu)}}\frac{W}{W^2 - 1}, V_0 = 0, V_{-1} = \pm\sqrt{\frac{R}{W(\lambda^2 - 4\mu)}}, V_1 = \pm\frac{1}{4}\frac{\sqrt{R(\lambda^2 - 4\mu)}}{W}$$

Substituting the values of case (1) into Eq. (9) then we achieve,

$$U_1(\xi) = \pm\sqrt{\frac{R}{W}}\frac{1}{(\lambda^2-4\mu)}\left|2\left\{tanh\left(\frac{\sqrt{\lambda^2-4\mu}}{2}\right)\xi\right\}^{-1} + \left(\lambda^2-4\mu\right)^2 tanh\left(\frac{\sqrt{\lambda^2-4\mu}}{2}\right)\xi\right| \tag{10}$$

$$U_2(\xi) = \pm\sqrt{\frac{R}{W}}\frac{1}{(\lambda^2-4\mu)}\left|2\left\{coth\left(\frac{\sqrt{\lambda^2-4\mu}}{2}\right)\xi\right\}^{-1} + \left(\lambda^2-4\mu\right)^2 coth\left(\frac{\sqrt{\lambda^2-4\mu}}{2}\right)\xi\right| \tag{11}$$

$$U_3(\xi) = \pm\sqrt{\frac{R}{W}}\left[\frac{1}{\sqrt{\lambda^2-4\mu}}\left\{\frac{4\xi^2+\lambda^2-4\mu}{4\xi}\right\}\right] \tag{12}$$

$$U_4(\xi) = \pm\sqrt{\frac{R}{W}}\frac{1}{\sqrt{\lambda^2-4\mu}}\left|2\left\{tan\left(\frac{\sqrt{4\mu-\lambda^2}}{2}\right)\xi\right\}^{-1} + \left(\lambda^2-4\mu\right)^2 tan\left(\frac{\sqrt{4\mu-\lambda^2}}{2}\right)\xi\right| \tag{13}$$

$$U_5(\xi) = \pm\sqrt{\frac{R}{W}}\frac{1}{\sqrt{\lambda^2-4\mu}}\left|2\left\{cot\left(\frac{\sqrt{4\mu-\lambda^2}}{2}\right)\xi\right\}^{-1} + \left(\lambda^2-4\mu\right)^2 cot\left(\frac{\sqrt{4\mu-\lambda^2}}{2}\right)\xi\right| \tag{14}$$

Case-2:

$$S = -\frac{2R}{W^2\lambda^2-4W^2\mu-\lambda^2+4\mu}, V_0 = 0,$$
$$V_{-1} = \pm\sqrt{\frac{2R}{W\left(\lambda^2-4\mu\right)}}i, V_1 = 0$$

Substituting the values of case (2) into Eq. (9) then we achieve,

$$U_6(\xi) = \pm\left[i\sqrt{\frac{R}{2W}}\left\{tanh\left(\frac{\sqrt{\lambda^2-4\mu}}{2}\right)\xi\right\}^{-1}\right] \tag{15}$$

$$U_7(\xi) = \pm\left[i\sqrt{\frac{R}{2W}}\left\{coth\left(\frac{\sqrt{\lambda^2-4\mu}}{2}\right)\xi\right\}^{-1}\right] \tag{16}$$

$$U_8(\xi) = \pm\left[i\sqrt{\frac{2R}{W\left(\lambda^2-4\mu\right)}}\xi\right] \tag{17}$$

$$U_9(\xi) = \pm\left[i\sqrt{\frac{R}{2W}}\left\{tan\left(\frac{\sqrt{4\mu-\lambda^2}}{2}\right)\xi\right\}^{-1}\right] \tag{18}$$

$$U_{10}(\xi) = \pm\left[i\sqrt{\frac{R}{2W}}\left\{cot\left(\frac{\sqrt{4\mu-\lambda^2}}{2}\right)\xi\right\}^{-1}\right] \tag{19}$$

Case-3:

$$S = -\frac{2R}{W^2\lambda^2-4W^2\mu-\lambda^2+4\mu}, V_0 = 0, V_{-1} = 0, V_1 = \pm\sqrt{\frac{R\left(4\mu-\lambda^2\right)}{8W}}$$

Substituting the values of case (3) into Eq. (9) then we achieve,

$$U_{11}(\xi) = \pm\left[\sqrt{\frac{R\left(4\mu-\lambda^2\right)}{8W}}\frac{\sqrt{\lambda^2-4\mu}}{2}\left\{tanh\left(\frac{\sqrt{\lambda^2-4\mu}}{2}\right)\xi^{-1}\right\}\right] \tag{20}$$

$$U_{12}(\xi) = \pm\left[\sqrt{\frac{R\left(4\mu-\lambda^2\right)}{8W}}\frac{\sqrt{\lambda^2-4\mu}}{2}\left\{coth\left(\frac{\sqrt{\lambda^2-4\mu}}{2}\right)\xi^{-1}\right\}\right] \tag{21}$$

$$U_{13}(\xi) = \pm\left[\sqrt{\frac{R\left(4\mu-\lambda^2\right)}{8W}}\xi^{-1}\right] \tag{22}$$

$$U_{14}(\xi) = \pm\left[\sqrt{\frac{R\left(4\mu-\lambda^2\right)}{8W}}\frac{\sqrt{\lambda^2-4\mu}}{2}\left\{tan\left(\frac{\sqrt{4\mu-\lambda^2}}{2}\right)\xi^{-1}\right\}\right] \tag{23}$$

$$U_{15}(\xi) = \pm\left[\sqrt{\frac{R\left(4\mu-\lambda^2\right)}{8W}}\frac{\sqrt{\lambda^2-4\mu}}{2}\left\{cot\left(\frac{\sqrt{4\mu-\lambda^2}}{2}\right)\xi^{-1}\right\}\right] \tag{24}$$

Case-4:

$$S = \pm\sqrt{\frac{R}{2W\left(\lambda^2-4\mu\right)}}\frac{W}{W^2-1}i, V_0 = 0, V_{-1} = \sqrt{\frac{R}{2W\left(\lambda^2-4\mu\right)}}i,$$
$$V_1 = -\frac{1}{8}\frac{R}{W}\sqrt{\frac{R}{2W\left(\lambda^2-4\mu\right)}}i$$

Substituting the values of case (4) into Eq. (9) then we achieve,

$$U_{16}(\xi) = \pm\frac{i}{2}\left\{tanh\left(\frac{\sqrt{\lambda^2-4\mu}}{2}\right)\xi\right\}^{-1}\left|\sqrt{\frac{R}{2W}} + \frac{1}{8}\frac{R}{W}\frac{1}{\sqrt{\frac{R}{2W\left(\lambda^2-4\mu\right)}}}\left(\sqrt{\lambda^2-4\mu}\right)\right| \tag{25}$$

$$U_{17}(\xi) = \pm\frac{i}{2}\left\{coth\left(\frac{\sqrt{\lambda^2-4\mu}}{2}\right)\xi\right\}^{-1}\left|\sqrt{\frac{R}{2W}} + \frac{1}{8}\frac{R}{W}\frac{1}{\sqrt{\frac{R}{2W\left(\lambda^2-4\mu\right)}}}\left(\sqrt{\lambda^2-4\mu}\right)\right| \tag{26}$$

$$U_{18}(\xi) = \pm i\left(1+\frac{R}{8W}\right)\left[\sqrt{\frac{R}{2W\left(\lambda^2-4\mu\right)}}\frac{1}{\xi}\right] \tag{27}$$

$$U_{19}(\xi) = \pm\frac{i}{2}\left\{tan\left(\frac{\sqrt{4\mu-\lambda^2}}{2}\right)\xi\right\}^{-1}\left|\sqrt{\frac{R}{2W}} + \frac{1}{8}\frac{R}{W}\frac{1}{\sqrt{\frac{R}{2W\left(\lambda^2-4\mu\right)}}}\left(\sqrt{\lambda^2-4\mu}\right)\right| \tag{28}$$

$$U_{20}(\xi) = \pm\frac{i}{2}\left\{cot\left(\frac{\sqrt{4\mu-\lambda^2}}{2}\right)\xi\right\}^{-1}\left|\sqrt{\frac{R}{2W}} + \frac{1}{8}\frac{R}{W}\frac{1}{\sqrt{\frac{R}{2W\left(\lambda^2-4\mu\right)}}}\left(\sqrt{\lambda^2-4\mu}\right)\right| \tag{29}$$

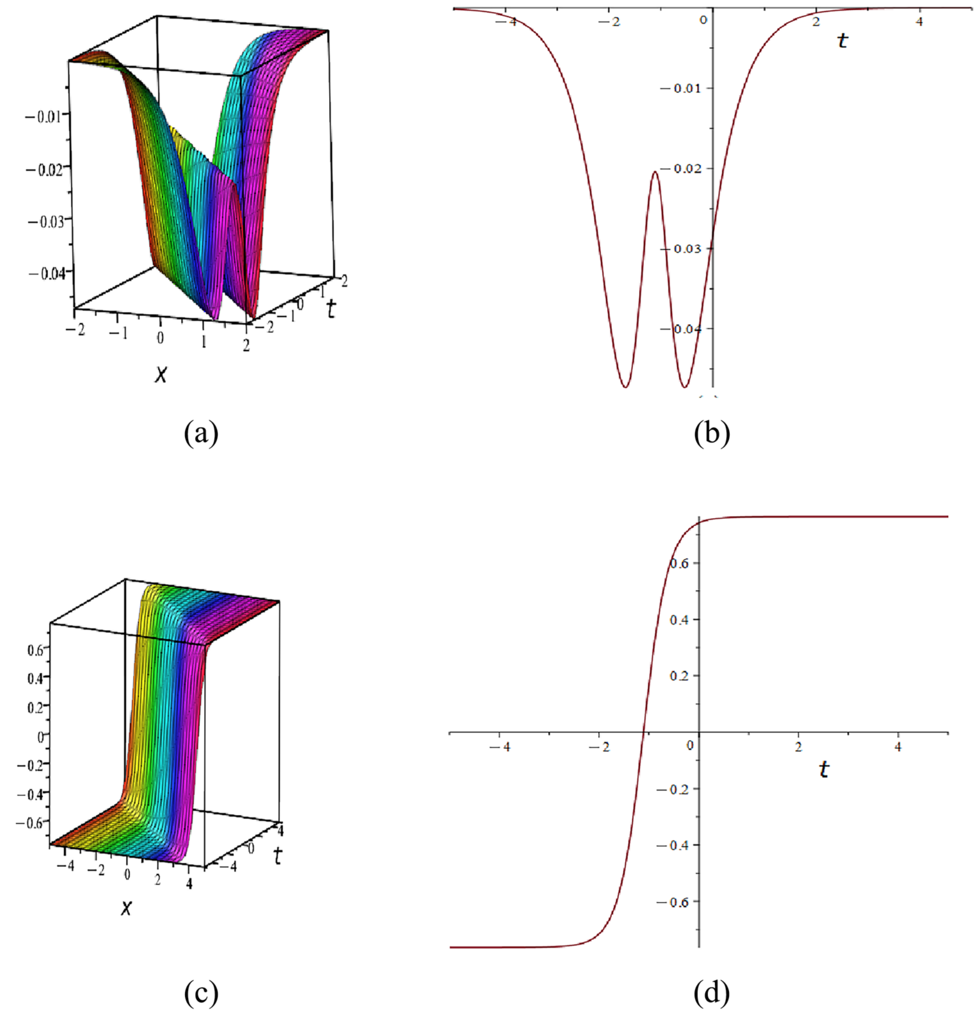

Fig. 1 The graphical representation of Eq. (11): **a** real 3D shape, **b** real 2D shape, **c** complex 3D shape, **d** complex 2D shape

4 Graphical representation

Graphs are a useful tool for advising and for calling problems' solutions calmly. A blueprint is a visible depiction of incomplete or imperfect solutions, or other data, typically used for allusive purposes. When assuming addition in routine activity, we need the fundamental capacity to use graphs effectively. We will discuss the graphical depiction of the discovered solutions in this section. Figure 1 exhibits the unique presentation of Eq. (11) using the parameters $\lambda = -4,\ \mu = 2,\ R = 2, W = 0.5, y = 0.5$. Specifically, Fig. 1 shows the 3D form (real and complex), 2D form (real and complex), and density form (real and complex) of Eq. (11). The real part of this shape addresses the wave profile, and complex part represents the anti-kink wave profile. The solution attributes of Eq. (10) are displayed in Fig. 2 using $\lambda = 3,\ \mu = 1,\ R = 0.5, W = -0.9, y = 0.5$. This shape addresses the bell shape and kink wave profile. The nature of the result of Eq. (13) is shown in Fig. 3 using $\lambda = 2,\ \mu = 2,\ R = 0.5, W = 0.9, y = 0.5$. This shape addresses the periodic wave profile. The solution attributes of Eq. (11) are displayed in Fig. 4 using $\lambda = 3,\ \mu = 1,\ R = 0.5, W = -0.9, y = 0.5$. This shape addresses cusp wave of multiple wings shape and kink wave profile.

5 Comparison

The paper compares the findings of the Zoomeron equation obtained by the proposed approach with solutions discovered in past research in this section.

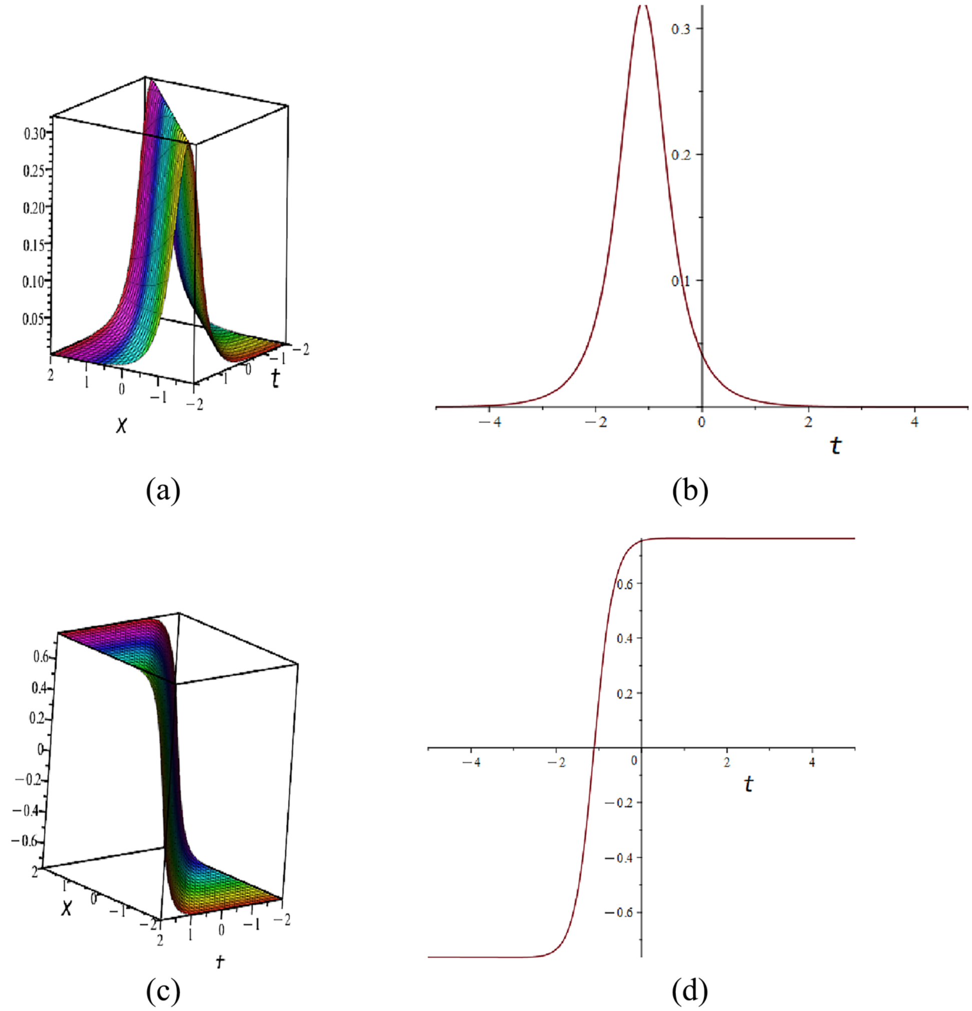

Fig. 2 The graphical representation of Eq. (10): **a** real 3D shape, **b** real 2D shape, **c** complex 3D shape, and **d** complex 2D shape

The comparison, as shown in Table, reveals differences between the obtained results and those documented by Reza Abazari et al. [30] obtained by $(G\prime/G)$–expansion method. The table shows that for some values of arbitrary parameters, the derived solutions deviate from those described in previous literature [30]. This highlights the consistency with previous results while emphasizing the novelty of the remaining outcomes. This work provides several innovative soliton solutions to the aforementioned equation utilizing the modified $(G\prime/G)$–expansion strategy, as illustrated by the comparison table below.

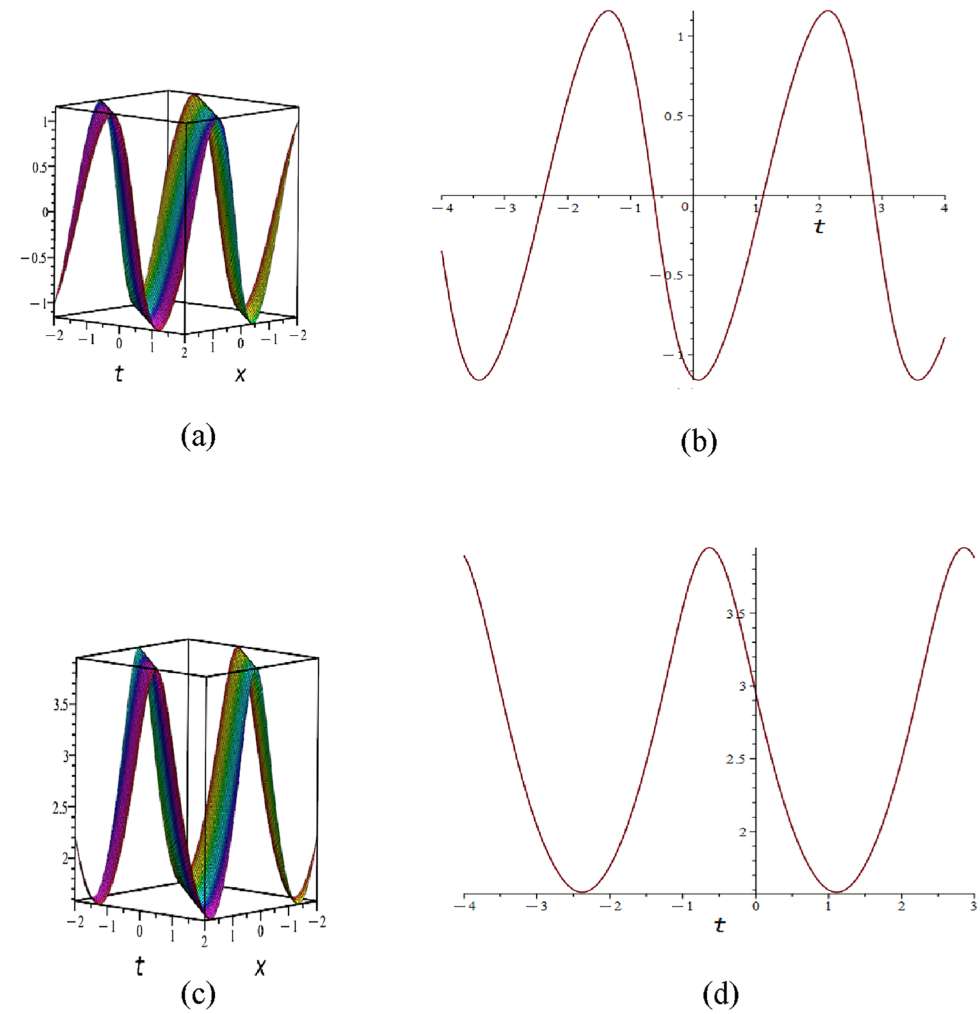

Fig. 3 The graphical representation of Eq. (13): **a** real 3D shape, **b** real 2D shape, **c** complex 3D shape, and **d** complex 2D shape

Solutions of Reza Abazari et al.[30]	Solutions attained in this study
(i) If $C_1^{\,2} > C_2^{\,2}$ then $u_H(\xi) = \pm\frac{1}{2}\sqrt{\frac{-2R}{w}}\tanh\left(-\frac{1}{2}\sqrt{\frac{2R}{c(w^2-1)}}(\xi-\eta_H)\right)$	(i) For case1 $U_1(\xi) = \pm\sqrt{\frac{R}{W}}\frac{1}{\sqrt{\lambda^2-4\mu}}\left[2\left\{tan\left(\frac{\sqrt{4\mu-\lambda^2}}{2}\right)\xi\right\}^{-1} + \left(\lambda^2-4\mu\right)^2 tan\left(\frac{\sqrt{4\mu-\lambda^2}}{2}\right)\xi\right]$
(ii) If $C_1^{\,2} < C_2^{\,2}$ then $u_H(\xi) = \pm\frac{1}{2}\sqrt{\frac{-2R}{w}}\coth\left(-\frac{1}{2}\sqrt{\frac{2R}{c(w^2-1)}}(\xi-\eta_H)\right)$	(ii) For case 2 $U_6(\xi) = \pm\left\lvert i\sqrt{\frac{R}{2W}}\left\{tanh\left(\frac{\sqrt{\lambda^2-4\mu}}{2}\right)\xi\right\}^{-1}\right\rvert$
(iii) For rational function $u_{rat}(\xi) = \pm\frac{c(w^2-1)C_2}{w(C_1+C_2\xi)\sqrt{-\frac{c(w^2-1)}{w}}}$	(iii) For case 3 $U_{11}(\xi) = \pm\left[\sqrt{\frac{R(4\mu-\lambda^2)}{8W}}\frac{\sqrt{\lambda^2-4\mu}}{2}\left\{tanh\left(\frac{\sqrt{\lambda^2-4\mu}}{2}\right)\xi^{-1}\right\}\right]$
	(iv) For case 4 $U_{16}(\xi) = \pm\frac{i}{2}\left\{tanh\left(\frac{\sqrt{\lambda^2-4\mu}}{2}\right)\xi\right\}^{-1}\left\lvert\sqrt{\frac{R}{2W}} + \frac{1}{8}\frac{R}{W}\frac{1}{\sqrt{\frac{R}{2W\left(\lambda^2-4\mu\right)}}}\left(\sqrt{\lambda^2-4\mu}\right)\right\rvert$

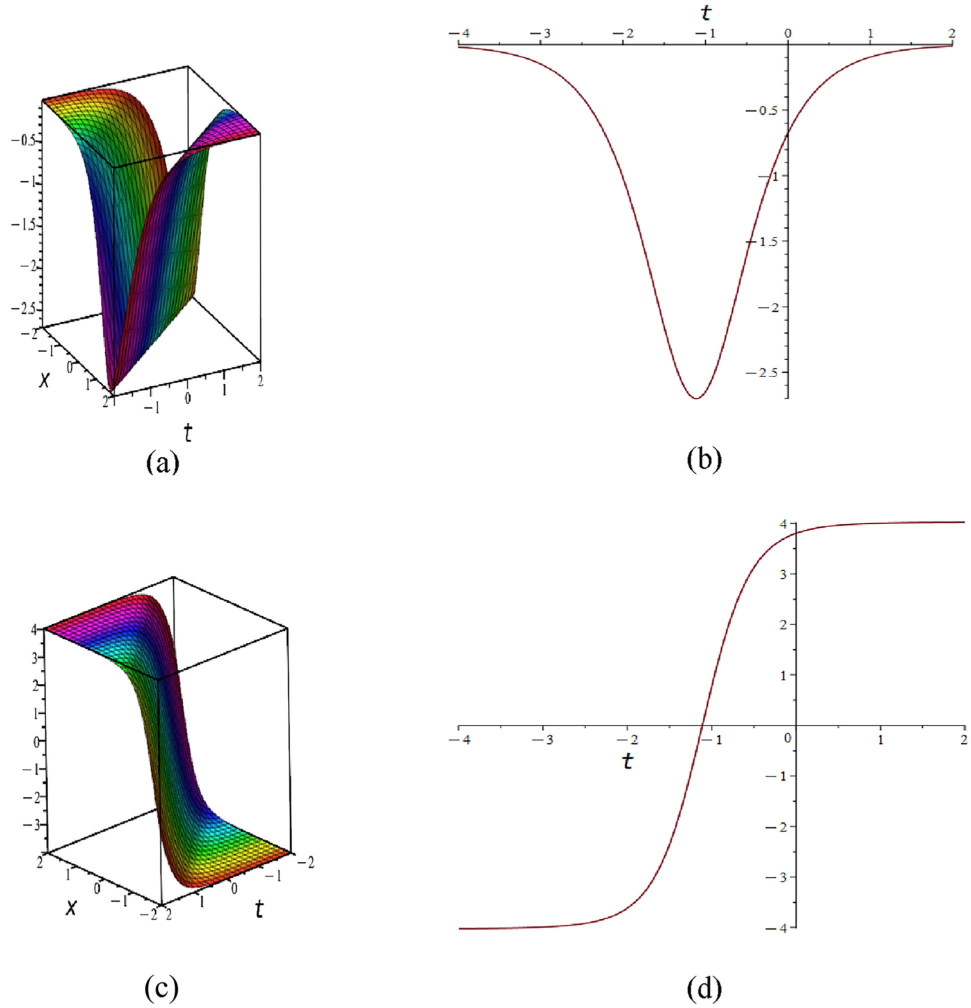

Fig. 4 The graphical representation of Eq. (11): (**a**) real 3D shape, (**b**) real 2D shape, (**c**) complex 3D shape, and (**d**) complex 2D shape

6 Conclusion

Our study thoroughly evaluated the innovative computational solutions related with the Zoomeron equation using the proposed approaches. We have shown a plethora of new computational outcomes over a spectrum encompassing hyperbolic, rational, and trigonometric equations, showing patterns such as the king-type form, singular king shape, periodic waves, and bell-shaped wave profiles. Utilizing Maple, this study employs the powerful capabilities of the software to present captivating two- and three-dimensional (2-D and 3-D) visual representations of these solutions. To emphasize the uniqueness of our study, we conducted comparison analyses, comparing our observed responses to those published in recent research papers. The demonstration of the efficacy of these established methodologies highlights its appropriateness, impact, and adaptability in dealing with various nonlinear models, necessitating additional investigation and inspection.

Author contributions All authors contributed to the study conception and design. Material preparation, Graphical Representation, Result discussion and analysis were performed by [SS], [RK], [AK] and [OS].The first draft of the manuscript was written by [SS], [RK], [PD] and all authors commented on previous versions of the manuscript. [PD] and [R.K] reviewed and edited the article. All authors read and approved the final manuscript.

Funding We did not receive any funding for this study.

Data availability This manuscript has no associated data.

Declarations

Conflict of interest The authors declare that they have no conflict of interest.

References

1. He J-H (2009) Nonlinear science as a fluctuating research frontier. Chaos Solitons Fractals 41(5):2533–2537. https://doi.org/10.1016/j.chaos.2008.09.027
2. Roshid MNAMAAHO (2015) Traveling wave solutions for fifth order (1+1)-dimensional Kaup–Keperschmidt equation with the help of exp(−Phi)-expansion method. Walailak J Sci Technol 12(11):1063–1073
3. Alam MN, Hafez MG, Ali Akbar M, Roshid H-O (2015) "Exact traveling wave solutions to the (3+1)-dimensional mKdV–ZK and the (2+1)-dimensional Burgers equations via exp(−Φ(η))-expansion method. Alex Eng J 54(3):635–644. https://doi.org/10.1016/j.aej.2015.05.005
4. Uddin S et al (2022) Bifurcation analysis of travelling waves and multi-rogue wave solutions for a nonlinear pseudo-parabolic model of visco-elastic Kelvin–Voigt fluid. Math Probl Eng 2022:1–16. https://doi.org/10.1155/2022/8227124
5. Osman MS, Rezazadeh H, Eslami M (2019) Traveling wave solutions for (3+1) dimensional conformable fractional Zakharov–Kuznetsov equation with power law nonlinearity. Nonlinear Eng 8(1):559–567. https://doi.org/10.1515/nleng-2018-0163
6. Korkmaz A, Hepson OE, Hosseini K, Rezazadeh H, Eslami M (2020) Sine-Gordon expansion method for exact solutions to conformable time fractional equations in RLW-class. J King Saud Univ Sci 32(1):567–574. https://doi.org/10.1016/j.jksus.2018.08.013
7. Hosseini K, Mirzazadeh M, Ilie M, Radmehr S (2020) Dynamics of optical solitons in the perturbed Gerdjikov–Ivanov equation. Optik Stuttg 206:164350. https://doi.org/10.1016/j.ijleo.2020.164350
8. Hosseini K, Mirzazadeh M, Vahidi J, Asghari R (2020) Optical wave structures to the Fokas–Lenells equation. Optik (Stuttg) 207:164450. https://doi.org/10.1016/j.ijleo.2020.164450
9. Aslan EC (2019) Optical soliton solutions of the NLSE with quadratic-cubic-Hamiltonian perturbations and modulation instability analysis. Optik (Stuttg) 196:162661. https://doi.org/10.1016/j.ijleo.2019.04.008
10. Ahmad H, Khan TA, Ahmad I, Stanimirović PS, Chu Y-M (2020) A new analyzing technique for nonlinear time fractional Cauchy reaction–diffusion model equations. Results Phys 19:103462. https://doi.org/10.1016/j.rinp.2020.103462
11. Ahmad H, Akgül A, Khan TA, Stanimirović PS, Chu Y-M (2020) New perspective on the conventional solutions of the nonlinear time-fractional partial differential equations. Complexity 2020:1–10. https://doi.org/10.1155/2020/8829017
12. Alam MN, Seadawy AR, Baleanu D (2020) Closed-form wave structures of the space–time fractional Hirota–Satsuma coupled KdV equation with nonlinear physical phenomena. Open Phys 18(1):555–565. https://doi.org/10.1515/phys-2020-0179
13. Khalid A, Rehan A, Nisar KS, Osman MS (2021) Splines solutions of boundary value problems that arises in sculpturing electrical process of motors with two rotating mechanism circuit. Phys Scr 96(10):104001. https://doi.org/10.1088/1402-4896/ac0bd0
14. Park C, Nuruddeen RI, Ali KK, Muhammad L, Osman MS, Baleanu D (2020) Novel hyperbolic and exponential ansatz methods to the fractional fifth-order Korteweg–de Vries equations. Adv Differ Equ 2020(1):627. https://doi.org/10.1186/s13662-020-03087-w
15. Ismail GM, Abdl-Rahim HR, Abdel-Aty A, Kharabsheh R, Alharbi W, Abdel-Aty M (2020) An analytical solution for fractional oscillator in a resisting medium. Chaos Solitons Fractals 130:109395. https://doi.org/10.1016/j.chaos.2019.109395
16. Yilmazer R, Osman MS, Ali KK (2022) 'Dynamic behavior of the (3+1)-dimensional KdV-Calogero–Bogoyavlenskii–Schiff equation. Opt Quantum Electron 54(3):160
17. Liu J-G, Zhu W-H, Osman MS, Ma W-X (2020) An explicit plethora of different classes of interactive lump solutions for an extension form of 3D-Jimbo–Miwa model. Eur Phys J Plus 135(5):412. https://doi.org/10.1140/epjp/s13360-020-00405-9
18. Zafar A et al (2021) Dynamics of different nonlinearities to the perturbed nonlinear Schrödinger equation via solitary wave solutions with numerical simulation. Fractal Fract 5(4):213. https://doi.org/10.3390/fractalfract5040213
19. Abbas A (2007) Finite element analysis of the thermoelastic interactions in an unbounded body with a cavity. Forsch Ingenieurwes 71:215–222
20. Alzahrani F (2020) An eigenvalues approach for a two-dimensional porous medium based upon weak, normal and strong thermal conductivities. Symmetry 12:113
21. Ibrahim RK, Abbas A (2016) 2D deformation in initially stressed thermoelastic half-space with voids. Steel Compos Struct 20(5):1103–1117
22. Ashraf Zenkour IAA (2014) Nonlinear transient thermal stress analysis of temperature-dependent hollow cylinders using a finite element model. Int J Struct Stabil Dyn 14(6):122
23. Abbas I, Hobiny A, Marin M (2020) Photo-thermal interactions in a semi-conductor material with cylindrical cavities and variable thermal conductivity. J Taibah Univ Sci 14(1):1369–1376. https://doi.org/10.1080/16583655.2020.1824465
24. Marin M (2021) The effects of fractional time derivatives in porothermoelastic materials using finite element method. Mathematics 9:32
25. Ma BFWX (1996) Explicit and exact solutions to a Kolmogorov–Petrovskii–Piskunov equation. Int J Non Linear Mech 31(3):329–338
26. Wen-Xiu Ma J-HL (2009) A transformed rational function method and exact solutions to the 3+1 dimensional Jimbo-Miwa equation. Chaos Solitons Fractals 42(3):1356–1363
27. Ma W-X (2021) N-soliton solution and the Hirota condition of a (2+1)-dimensional combined equation. Math Comput Simul 190:270–279
28. Ma W-X (2023) Four-component integrable hierarchies of Hamiltonian equations with (m+n+2)th-order Lax pairs. Theor Math Phys 216(2):1180–1188
29. Ma W-X (2023) A six-component integrable hierarchy and its Hamiltonian formulation. Mod Phys Lett B 37(32):14
30. Abazari R (2011) The solitary wave solutions of Zoomeron equation. Appl Math Sci 5(59):2943–2949